5

Complexity and Heterogeneity in MOFs

5.1 Introduction

Thus far, we have described metal-organic framework (MOF) structures that are built from two different building units, where one kind of a linker and one kind of a secondary building unit (SBU) are linked into a periodic framework structure. It is however possible to combine more than two kinds of building unit together into a single framework. For this scenario, we distinguish two cases: "complexity" and "heterogeneity." This will be the focus of this chapter and we begin by illustrating the difference between heterogeneity and complexity based on examples of MOF structures, all involving $Zn_4O(–COO)_6$ SBUs, but different organic linkers.

When $Zn_4O(–COO)_6$ SBUs are reticulated with linear ditopic BDC or trigonal tritopic BTB linkers, MOF-5 (**pcu**) or MOF-177 (**qom**) are formed, respectively [1]. In contrast, when both linkers are employed in the same synthesis, a different and more complex MOF structure (**muo**, UMCM-1, $Zn_4O(BDC)(BTB)_{4/3}$) results [2]. Notice that in this multinary structure the position of each of the individual building units is crystallographically defined (Figure 5.1) and we refer to this as "complexity within frameworks." Such complexity can be achieved by introducing (i) multiple different linkers, (ii) multiple different SBUs, (iii) multiple different SBUs and linkers, or (iv) ordered vacancies into a single MOF structure.

A different scenario arises when $Zn_4O(–COO)_6$ SBUs are reticulated with linear ditopic BDC or Br-BDC linkers. Here, two isostructural and metrically identical but chemically distinct MOFs, MOF-5 (**pcu**) and IRMOF-2 (**pcu**), respectively, are formed [3]. Since the backbone of both MOFs is identical, it is possible to combine both linkers within one framework while maintaining the parent structure type (**pcu**). Notice that in the resulting structure (MTV-MOF-5) the spatial arrangement of the BDC and Br-BDC linkers is unknown, thus introducing heterogeneity onto the otherwise ordered MOF-5 backbone (Figure 5.2), and we refer to this as "heterogeneity in frameworks" [4]. Heterogeneity can be achieved by introducing (i) multiple interchangeable linkers that are identical in terms of their binding groups and metrics but different with respect to their chemical composition, (ii) multiple metal ions that form the same SBU, and (iii) aperiodic vacancies onto or into the backbone of a single MOF structure. Such MOFs are referred to as multivariate (MTV) MOFs.

Introduction to Reticular Chemistry: Metal-Organic Frameworks and Covalent Organic Frameworks,
First Edition. Omar M. Yaghi, Markus J. Kalmutzki, and Christian S. Diercks.

Companion website: www.wiley.com/go/yaghi/reticular

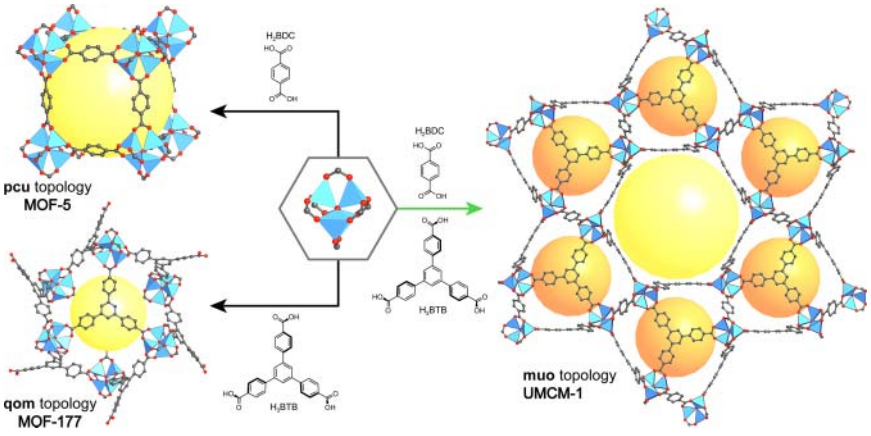

Figure 5.1 Complexity in frameworks is observed in multinary MOFs, where three or more building units of different size and geometry are combined into a single MOF structure. In this example, we consider the reticulation of $Zn_4O(–COO)_6$ SBUs with H_2BDC and H_3BTB linkers. In the binary systems, the products of these reticulations are MOF-5 (**pcu**) and MOF-177 (**qom**), respectively. In contrast, reticulating both linkers with $Zn_4O(–COO)_6$ SBUs into a single MOF structure yields UMCM-1 (**muo**), a MOF that is structurally not related to any of the two binary structures. Since this MOF has a more complex backbone, we refer to this as "complexity in frameworks." All hydrogen atoms are omitted for clarity. Color code: Zn, blue; C, gray; O, red.

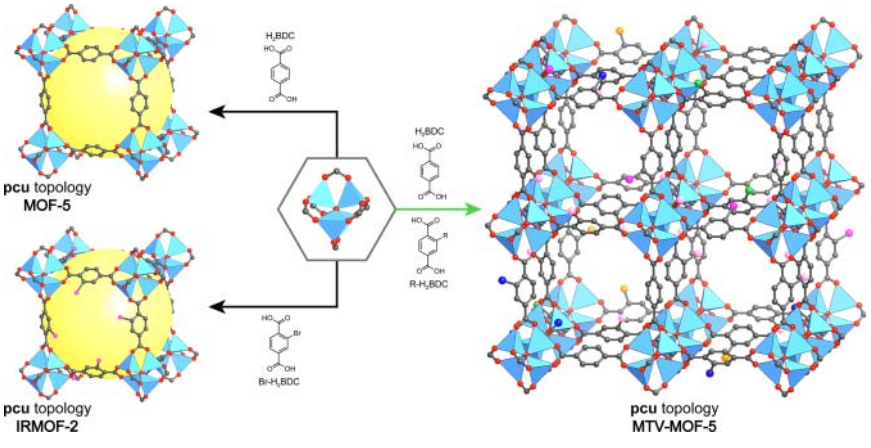

Figure 5.2 Heterogeneity in frameworks is observed, when three or more building units, of which at least two are structurally interchangeable, are reticulated into a single framework. In this example, we consider the reticulation of $Zn_4O(–COO)_6$ SBUs with H_2BDC and Br-H_2BDC linkers. In the binary systems, the products of these reticulations are MOFs of the same **pcu** topology, MOF-5 and IRMOF-2, respectively. MOF-5 and IRMOF-2 are isoreticular (isostructural) but differ in terms of their chemical composition. Thus, reticulating both linkers with $Zn_4O(–COO)_6$ SBUs into a single structure again yields a MOF (MTV-MOF-5) of the same structure type (**pcu**). The spatial arrangement of the BDC and Br-BDC linker in MTV-MOF-5 imposes heterogeneity onto its crystalline backbone, which is thus referred to as "heterogeneity in frameworks." All hydrogen atoms are omitted for clarity. Color code: Zn, blue; C, gray; O, red; Br, pink; Undefined substituents of the R-BDC linkers in MTV-MOF-5 have been given various colors.

In this chapter, we explore MOF structures that go beyond binary systems and illustrate how complexity and heterogeneity within frameworks can afford MOFs with properties that go beyond those of the corresponding binary counterparts.

5.2 Complexity in Frameworks

5.2.1 Mixed-Metal MOFs

Introducing multiple different SBUs into a MOF structure expands the scope of accessible net topologies. In the case of MOF structures containing two geometrically and/or metrically distinct SBUs, these are (i) either all constructed from the same metal or (ii) different metals that from distinct SBUs within the same material. Forming multiple distinct types of SBU in a one-pot reaction poses a challenge because, as discussed in Chapters 3 and 4, meticulously adjusted reaction conditions are required to target the formation of a specific SBU. Thus, in many cases, MOF structures with more than one unique SBU are formed by chance rather than by design. In the following text we will discuss two general approaches for the synthesis of complex MOF structures built from more than one type of SBU.

5.2.1.1 Linker De-symmetrization

The approach of "vertex-directed linker de-symmetrization" is used in the design and synthesis of UMCM-150 ($Cu_3(BHTC)_2(H_2O)_3$), a MOF built from two different SBUs, the 4-c $Cu_2(–COO)_4$ paddle wheel and the comparatively rare 6-c $Cu_3(–COO)_6$ paddle wheel (Figure 5.3) [5]. The de-symmetrized trigonal H_3BHT linker (C_{2h}) is made by asymmetric expansion of the trigonal H_3BTC linker (D_{3h}). In the structure of UMCM-150, each BHTC linker is connected to one 6-c and two 4-c paddle wheel SBUs and the resulting framework has an overall **agw** topology. As depicted in Figure 5.3, the 3,4,6-connected **agw** net consists of triangles (BHTC), squares ($Cu_2(–COO)_4$), and trigonal prisms ($Cu_3(–COO)_6$). Dissecting the BHTC linker into a benzoate and isophthalate subunit reveals that the structure of UMCM-150 can alternatively be described as hexagonal kagome (**kgm**, the augmented net of **kgm** is called **fxt**) layers built from 4-c paddle wheel SBUs connected through ditopic isophthalate units that are sixfold cross-linked through the 6-c trigonal prismatic paddle wheel units to give a 3D framework.

5.2.1.2 Linkers with Chemically Distinct Binding Groups

To gain more control over the reticulation process when targeting complex MOF structures, linkers bearing multiple different binding groups favoring the formation of different types of SBU can be used. This approach is employed in the synthesis of MOF-325 where reticulating Cu^{2+} ions and H_2PyC (4-pyrazolecarboxylic acid) yields a framework of the chemical formula $Cu_3(H_2O)_3[(Cu_3O)(PyC)_3(NO_3)L_2]_2$ (Figure 5.4) [6]. This framework contains two different types of SBU. Trigonal planar $Cu_3OL_3(PyC)_3$ SBUs (L = NO_3 and/or solvent, PyC = 4-pyrazolecarboxylate) are formed by the pyrazolate portion of PyC, and the carboxylates connect two Cu^{2+} centers to form

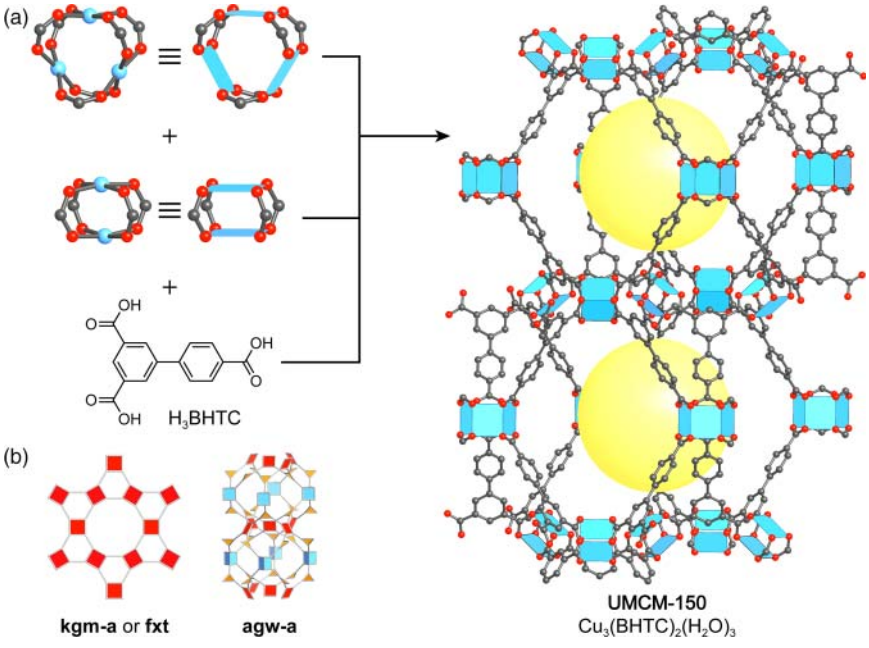

Figure 5.3 (a) Crystal structure of UMCM-150. In this example, vertex-directed linker de-symmetrization directs the synthesis toward the formation of two distinct SBUs; a 4-c and a 6-c copper paddle wheel. The resulting structure can be described as kagome layers (**kgm**) formed from 4-c paddle wheel SBUs and the isophthalate portion of the BHTC linker, that are triply cross-linked to form a 3D structure of **agw** topology. (b) Topology representations of the augmented **kgm** (**fxt**) and **agw** net, the 4-c paddle wheel SBUs are represented by red squares, the 6-c paddle wheel SBUs by blue trigonal prisms, and the BHTC linkers by orange triangles. All hydrogen atoms are omitted for clarity. Color code: Cu, blue; C, gray; O, red.

$Cu_2(–COO)_4$ paddle wheel SBUs [6]. Consequently, these trigonal planar and square planar SBUs form a framework of **tbo** topology. MOF-325 is isostructural to HKUST-1, where the trigonal planar BTC (benzene-tricarboxylate) linkers (D_{3h}) are replaced by trigonal planar $Cu_3OL_3(PyC)_3$ SBUs (D_{3h}). Since these trinuclear $Cu_3OL_3(PyC)_3$ SBUs are larger than the BTC linker in HKUST-1, the pores of MOF-325 (19.6 Å) are also larger than those in the structure of HKUST-1 (18 Å) [7].

To prepare even more complex framework structures, the linker used in the synthesis of MOF-325 (i.e. H_2PyC) is reticulated with two different metals to enforce the formation of two distinct types of SBU. Reticulation of H_2PyC with Cu^{2+} and Zn^{2+} ions facilitates the formation of a highly complex MOF structure (FDM-3, where FDM = Fudan Materials) of chemical formula $[(Zn_4O)_5(Cu_3OH)_6(PyC)_{22.5}(OH)_{18}(H_2O)_6][Zn(OH)(H_2O)_3]_3$ [8]. The structure of FDM-3 contains multiple different types of SBU; one copper-based $Cu_3OH(–PyC)_3$ SBU and six different zinc-based SBUs that are structurally related to the $Zn_4O(–COO)_6$ SBU. Four of these zinc-based SBUs are octahedral ($ZnO_4(–COO)_3R_3$ where R = –COO or –NN) and two are square pyramidal ($ZnO_4(–COO)_4R$). The highly complex structure of FDM-3 crystallizes in the

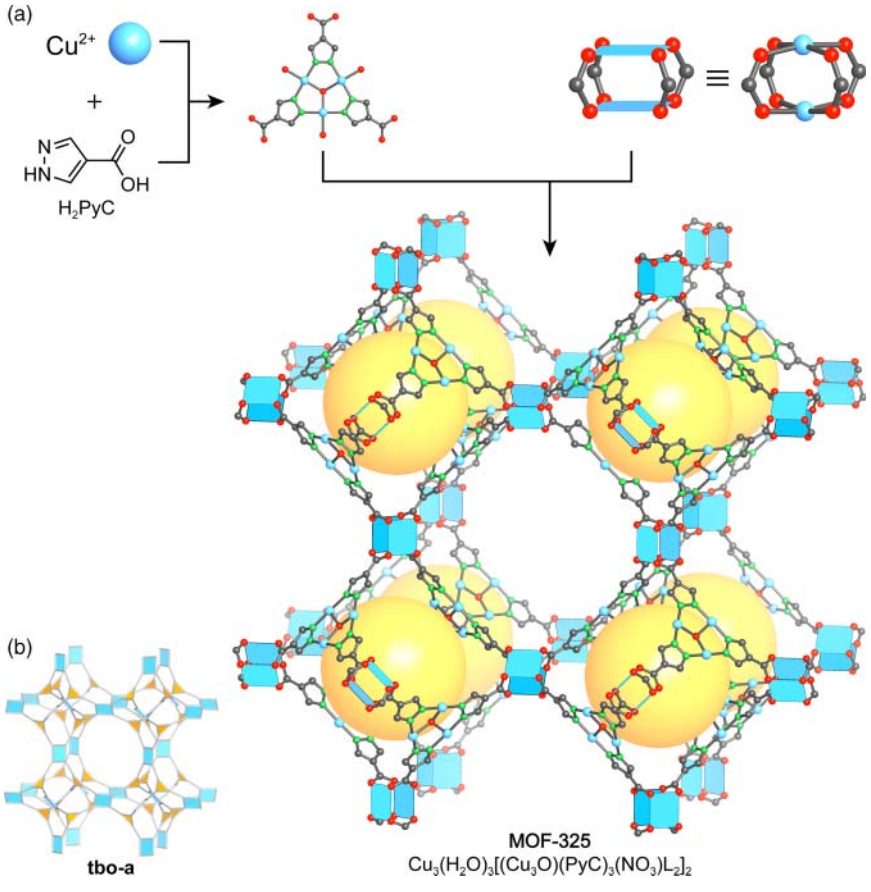

Figure 5.4 (a) Two distinct copper SBUs sustain the structure of MOF-325. The trigonal 3-c $Cu_3OL_3(PyC)_3$ SBU has D_{3h} symmetry and connects 4-c paddle wheel SBUs to form a framework of **tbo** topology. The large pores (19.6 Å) are connected in all three directions giving rise to a 3D intersecting pore system. (b) Representation of the augmented **tbo** net. Copper paddle wheel SBUs are represented by blue squares and $Cu_3OL_3(PyC)_3$ units are represented by orange triangles. The terminal water ligands on the copper paddle wheel, terminal ligands on the $Cu_3OL_3(PyC)_3$ SBUs, and all hydrogen atoms are omitted for clarity. Color code: Cu, blue; N, green; C, gray; O, red.

3,5,6-connected **ott** net (Figure 5.5) and the pores of the anionic framework are partially filled with charge balancing $[Zn(OH)(H_2O)_3]^+$ ions.

The overall structure of FDM-3 is composed of four kinds of cage, two of which are microporous and the other two are mesoporous (Figure 5.6). The cubic cage (cage I) has a diameter of 7.6 Å and is positioned at the center and on all edges of the cubic unit cell similar to a cubic close packed arrangement. The second cage (cage II) can be described by a gyrobifastigium (two face-regular trigonal prisms rotated toward each other by 90° and joined along corresponding square faces) and has a size of approximately 8.0×8.0 Å. The mesoporous cage III is topologically identical to the largest cage in MIL-101 and has a pore diameter of 23.4 Å. Cage IV, is the largest cage in FDM-3. It is of pseudo-octahedral shape

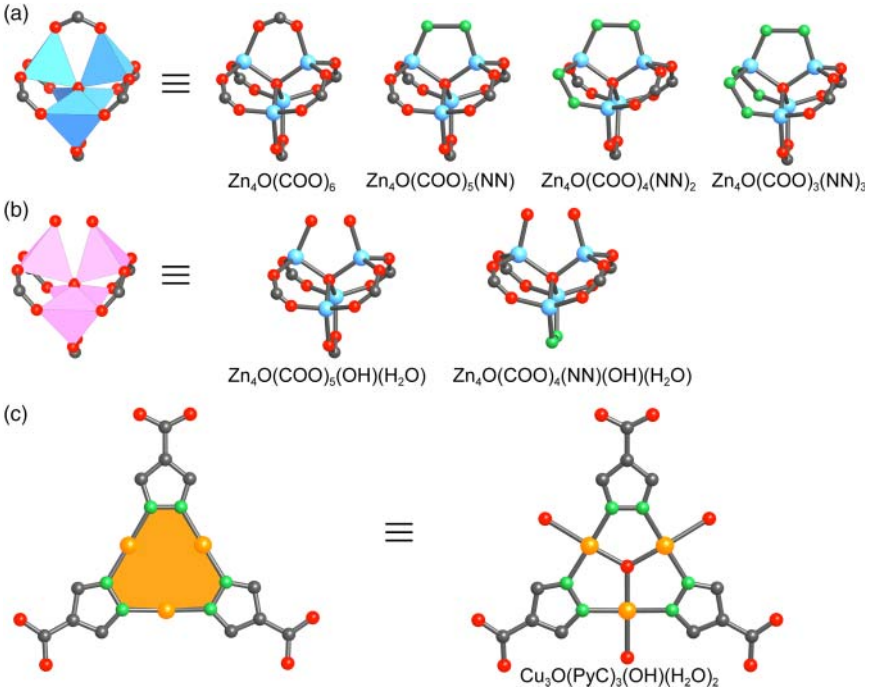

Figure 5.5 The structure of FDM-3 contains seven different types of SBU that are built from two different metals (zinc and copper) and have a connectivity ranging from 3 to 6. (a) 6-c octahedral zinc-based SBUs (blue) of chemical formula $Zn_4O(COO)_6$, $Zn_4O(COO)_5(NN)$, $Zn_4O(COO)_4(NN)_2$, and $Zn_4O(COO)_4(NN)_3$. (b) 5-c square pyramidal zinc-based SBUs (pink) of chemical formula $Zn_4O(COO)_5(OH)(H_2O)$ and $Zn_4O(COO)_4(NN)(OH)(H_2O)$. (c) 3-c trigonal copper-based SBU (orange) of chemical formula $Cu_3(OH)(H_2O)_2(PyC)_3$. All hydrogen atoms are omitted for clarity. Color code: Zn, blue; Cu, orange; C, gray; N, green; O, red.

and has a pore diameter of 28.8 Å. One single unit cell of FDM-3 contains a total of 28 microporous cages (4 × cage I, 24 × cage II) and 11 mesoporous cages (8 × cage III, 3 × cage IV) and the fully activated materials has a surface area of 2585 $m^2\ g^{-1}$.

5.2.2 Mixed-Linker MOFs

Similar to the synthesis of MOFs built from more than one kind of SBU, employing more than one kind of linker in a MOF synthesis can result in the formation of a complex multinary MOF structure. It is however difficult to synthesize such MOFs in a designed way, because the presence of multiple building units in the reaction mixture introduces a degree of unpredictability. To illustrate this, we look at the example used in the beginning of this chapter: MOF structures that are formed by the reticulation of Zn^{2+} ions with linear ditopic H_2BDC and/or trigonal tritopic H_3BTB (see Figure 5.1). The reticulation of Zn^{2+} ions with H_3BTB leads to the formation of MOF-177 (**qom**), and under almost identical conditions, reticulation of Zn^{2+} with H_2BDC yields MOF-5 (**pcu**).

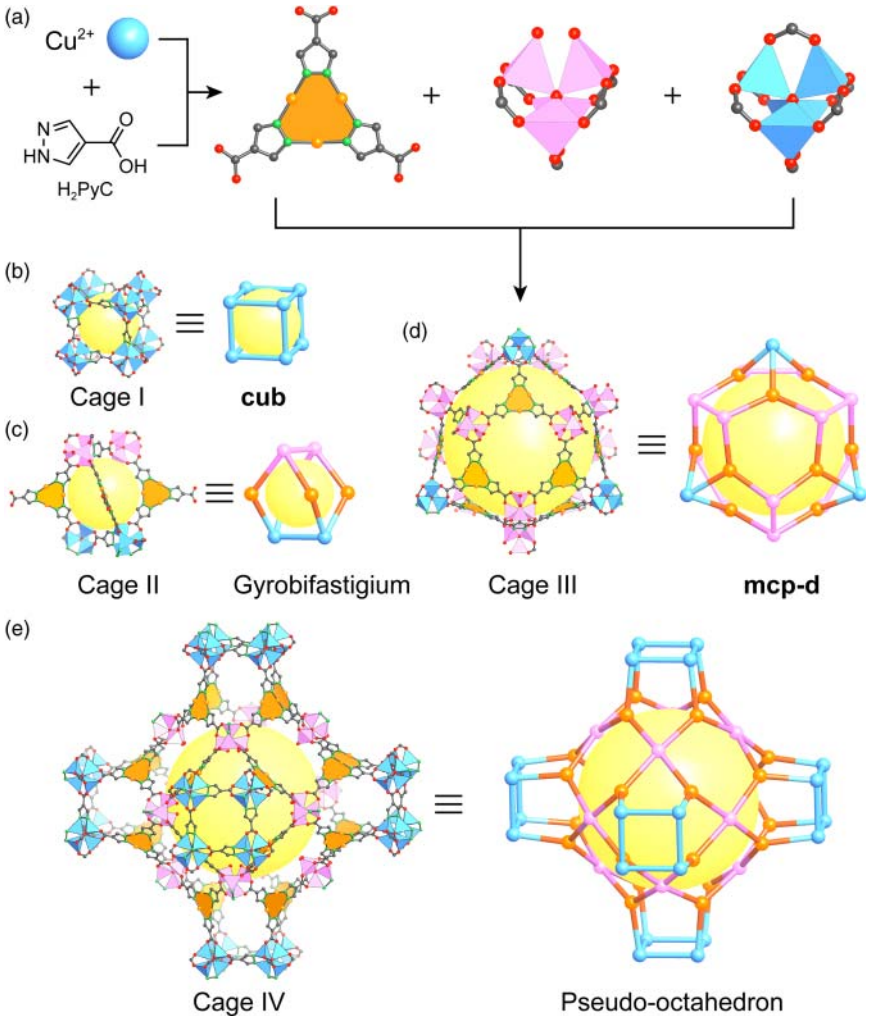

Figure 5.6 (a) The combination of the seven different types of SBUs shown in Figure 5.5 within one MOF structure (FDM-3) gives a highly complex framework structure with **ott** topology. The structure contains four differently sized cages; two micro- and two mesoporous. (b) Cage I (**cub**) is built from only one type of SBU, has a diameter of 7.8 Å, and resembles the pores in the structure of MOF-5. (c) Cage II has the shape of a gyrobifastigium and is about 8.0 × 8.0 Å large. (d) Cage III is of **mcp-d** topology and measures 23.4 Å in diameter. (e) The largest cage (cage IV) is of pseudo-octahedral shape, is built from 60 SBUs, and has a diameter of 28.8 Å. A single unit cell of FDM-3 contains a total of 39 cages (4 × cage I, 24 × cage II, 8 × cage III, and 3 × cage IV).

In contrast, for a synthesis involving both linkers, it is not yet possible to predict whether one or the other binary MOF, or even a new complex mixed-linker MOF will form. Studies of the ternary system $Zn^{2+}/H_2BDC/H_3BTB$ reveal that by altering the ratio of linkers, MOF-5, MOF-177, and a mixed-linker MOF (UMCM-1, $Zn_4O(BDC)(BTB)_{4/3}$, **muo**), that contains both linkers can be isolated (Figure 5.7) [9].

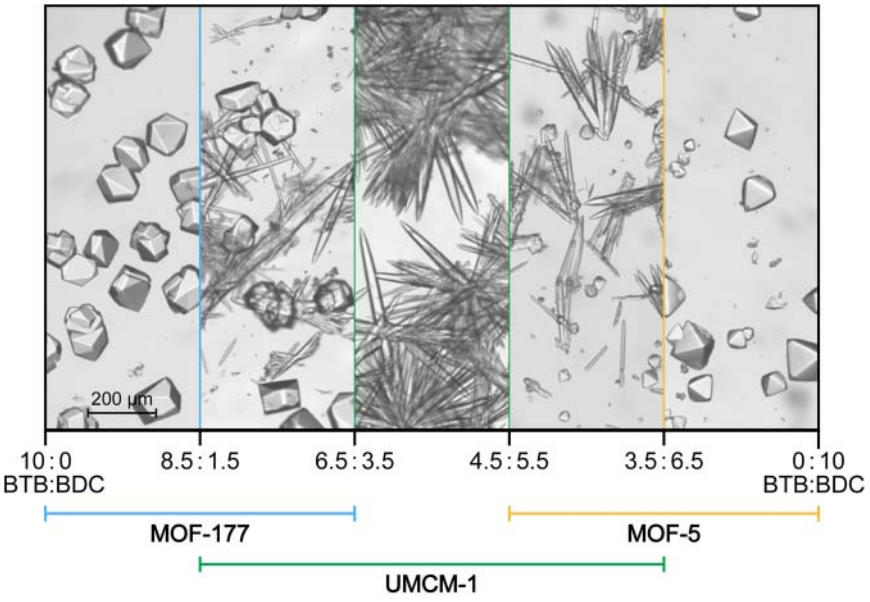

Figure 5.7 Formation of different MOF phases depending on the ratio of the linkers (H_2BDC:H_3BTB) employed in the synthesis. MOF-5 (**pcu**) and MOF-177 (**qom**) are formed from the reaction of Zn^{2+} and only one (or an excess of one) linker, while for the reaction with linker mixtures with a ratio of H_2BDC:H_3BTB between 6 : 4 and 4 : 6 the formation of phase pure UMCM-1 (**muo**) is observed.

In the structure of UMCM-1, each octahedral $Zn_4O(–COO)_6$ SBU is connected to two BDC and four BTB linkers resulting in cages of about 14×17 Å, each constructed from nine SBUs connected through six BDC and five BTB linkers (Figure 5.8). These cages are fused in an edge-sharing manner to form an arrangement with 1D hexagonal channels of 24×29 Å in diameter. UMCM-1 combines both, the high surface area ($5730\ m^2\ g^{-1}$) common to most MOFs and the large pore apertures common to mesoporous silicates/aluminosilicates. Efforts to prepare an expanded version of UMCM-1 (**muo**) by replacing H_2BDC with H_2T^2DC (thieno[3,2-*b*]thiophene-2,5-dicarboxylate) have resulted in the formation of a framework with a different structure, termed UMCM-2 ($Zn_4O(T^2DC)(BTB)_{4/3}$, **umt** topology) [10]. When both, the geometry and the metrics (length ratios) of all constituents is maintained, the isoreticular expansion of multinary MOFs is feasible, as exemplified by the expansion of UMCM-2 to DUT-32 ($Zn_4O(BPDC)(BTCTB)_{4/3}$) [11].

In a similar fashion, another mixed-linker MOF can be prepared by reticulation of Zn^{2+} ions with trigonal tritopic H_3BTE and linear ditopic H_2BPDC linkers. The use of Zn^{2+} ions and H_2BPDC or H_3BTE separately yields the binary MOFs IRMOF-10 (**pcu**) and MOF-180 (**qom**), respectively [1, 3]. Combining both of these linkers within one structure results in a multinary framework of chemical formula $(Zn_4O)_3(BPDC)_4(BTE)_3$) named MOF-210 (Figure 5.9), that crystallizes in a **toz** topology [1]. This is especially interesting, considering that UMCM-1 is built from building units that are represented by the same general vertex figures (octahedron, triangle, and linear edge) but are differ with respect to their metrics. The structure of MOF-210 contains two distinct cages, where the larger

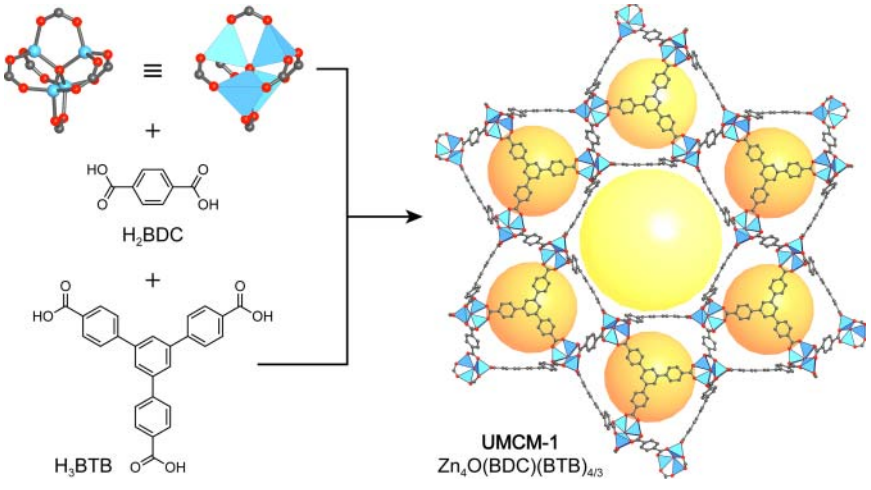

Figure 5.8 Crystal structure of UMCM-1 with underlying **muo** topology.Small cages of about 14 × 17 Å (orange spheres) are formed by linking nine SBUs through six BDC and five BTB linkers. These small cages are arranged in an edge-sharing manner to create large 1D hexagonal channels of 24 × 29 Å (yellow sphere). All hydrogen atoms are omitted for clarity. Color code: Zn, blue; C; gray; O, red.

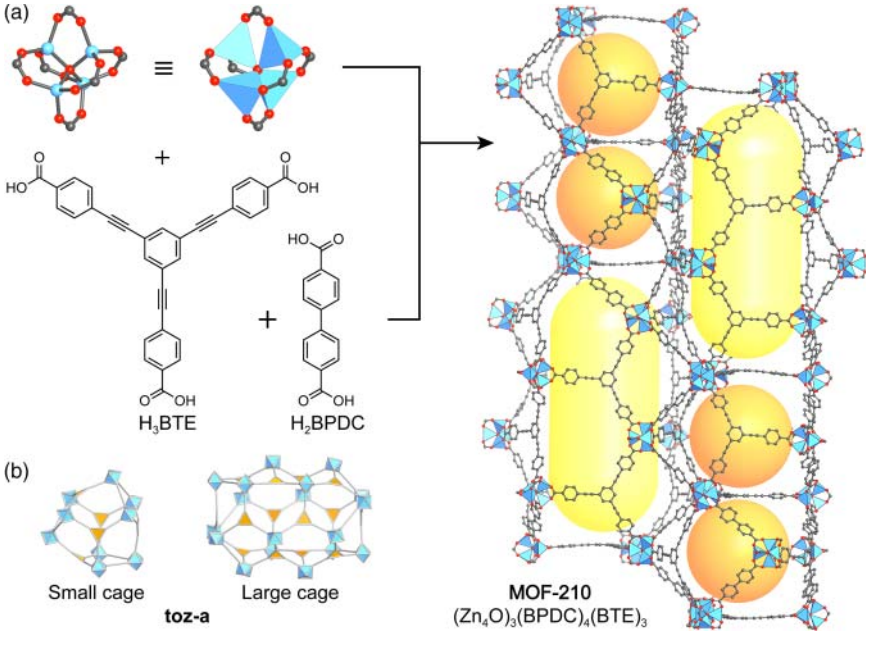

Figure 5.9 (a) Crystal structure of MOF-210. Reticulation of Zn^{2+} ions with H_3BTE and H_2BPDC leads to the formation of a complex framework structure with **toz** topology. The structure comprises two differently sized pores. The smaller pores (orange spheres) have a diameter of approximately 11 Å, and the larger elliptical pores (yellow ellipsoids) measure 27 × 48 Å. This complex architecture gives rise to an ultrahigh surface area of 6240 $m^2\ g^{-1}$. (b) Topology representation of the two cages in the **toz** net of MOF-210: BTE linkers are represented by orange triangles and zinc SBUs are shown as blue octahedra. All hydrogen atoms are omitted for clarity. Color code: Zn, blue, C, gray; O, red.

cage comprises 18 $Zn_4O(–COO)_6$ SBUs connected by 14 BTE and 6 BPDC linkers, encompassing an elliptical pore of about 27×48 Å. The smaller cage has a diameter of approximately 11 Å and is framed by 9 $Zn_4O(–COO)_6$ SBUs, 5 BTE, and 6 BPDC linkers. The complex framework architecture of MOF-210 gives rise to an ultrahigh surface area of 6240 m^2 g^{-1} and outstanding gas sorption properties.

All mixed-linker MOFs discussed thus far are built from a combination of trigonal tritopic and linear ditopic linkers, and $Zn_4O(–COO)_6$ SBUs, but they all crystallize in different structure types. This highlights the fact that for multinary systems, the *a priori* design is not trivial. An exact ratio of the linker lengths must be maintained to direct the reticular synthesis toward a specific topology as illustrated by the subtle variations in the linker length ration between MOF-210 (0.76), UMCM-1 (0.786), and UMCM-2 (0.79). This makes the isoreticular expansion of such structures challenging and sometimes even impossible as in the case of MOF-205 ($Zn_4O(BTB)_{4/3}(NDC)$) [1].

Multinary MOFs can also be built from more than three distinct building units, and several MOFs combining three different kinds of linker within a single structure are known. Among them are MOFs with pillared-layered structures. In MOFs of that type most often only the 2D layers are formed by joining the SBUs through carboxylate-based linkers and the pillars are typically O- or N-donor linkers (e.g. 4,4′-bipyridine, DABCO), and similar structures containing only carboxylate-based linkers are rare. An example of such frameworks is a series of isoreticular MOFs based on UMCM-4, a quaternary pillared-layered MOF where all building units are stitched together solely by strong bonds. In all structures (UMCM-4, 10, 11, 12), $Zn_4O(–COO)_6$ SBUs are connected by tritopic TPA and ditopic BDC linkers to form layers with a **cru** topology. These layers are in turn pillared by BDC (UMCM-4), Me_4-BPDC (UMCM-10, Me4-BPDC = 2,2′,6,6′-tetramethylbiphenyl-4,4′-dicarboxylic acid), EDDB (UMCM-11, EDDB = 4,40-(ethyne-1,2-diyl)dibenzoic acid), or TMTPDC (UMCM-12, TMTPDC = 2′,3′,5′,6′-tertramethylterphenyl-4,4″-dicarboxylic acid) to give rise to 3D extended framework structures [12]. In contrast to other mixed-linker systems that do not possess a pillared-layered structure, here, an anisotropic isoreticular expansion is possible by design. Introduction of a longer ditopic linker into the 2D layers leads to a disturbance of their symmetry, which is why selective implementation of the expanded ditopic linkers is only observed between the layers. The tunability of the pore window by expansion of the linker is a powerful tool for tweaking the selectivity in molecular sieving.

Another example for a complex, yet well-ordered, quaternary 3D framework is MUF-7a ($(Zn_4O)_3$ $(BTB)_{4/3}(BDC)_{1/2}(BPDC)_{1/2}$, MUF = Massey University Metal-Organic Frameworks) with an underlying **ith-d** topology [13]. MUF-7a is formed by reticulation of Zn^{2+} ions with trigonal tritopic H_3BTB, linear ditopic H_2BDC, and linear ditopic H_2BPDC linkers. Its structure has two different cages that measure 10 and 20 Å in diameter (Figure 5.10). The precise design of the linker and matching of its symmetry to that of the sites it occupies in the crystal structure helps to avoid randomness and disorder. This approach allows for the synthesis of MOFs with "programmed pores," featuring multiple functional

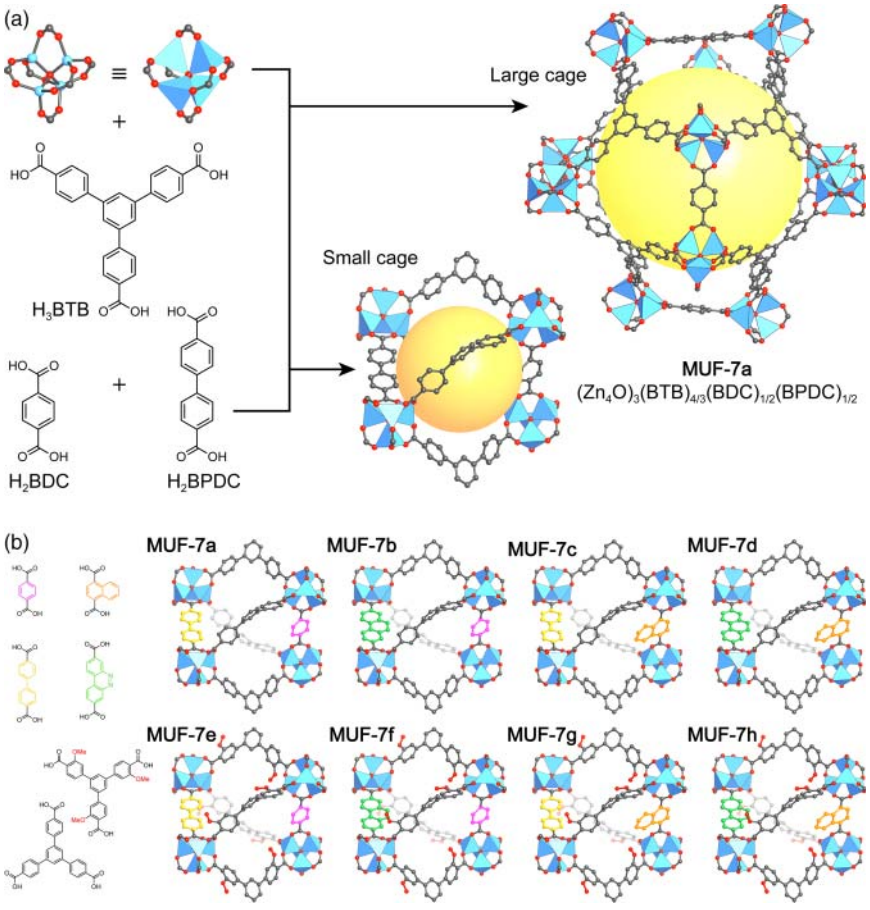

Figure 5.10 (a) Fragments of the crystal structure of the quaternary MOF MUF-7a showing the small (orange sphere) and large pore (yellow sphere) that assemble to form a framework with an overall **ith-d** topology (not shown). (b) Employing derivatized linkers that are symmetry matched to their respective positions within the crystal structure allows for the formation of eight different isoreticular materials (MUF-7a-h) with programmed pores. Only the small tetrahedral pores are shown. BTB and $(OMe)_3$-BTB linkers are only shown partially and all other derivatized linkers are highlighted in different colors. All hydrogen atoms are omitted for clarity. Color code if not noted differently: Zn, blue; C, gray; O, red.

groups arranged in a predetermined pattern within the periodic lattice. MUF-7 analogs with programmed pores show an enhancement of the CO_2 adsorption capacity by almost 100% [14].

Sequential linker installation (SLI) is another approach to the synthesis of MOFs with highly complex structures, albeit less generally applicable [15]. SLI allows for the systematic increase of the connectivity of SBUs making it possible to prepare frameworks that cannot be synthesized directly. This approach is discussed in more detail in Chapter 6 in the context of the post-synthetic modification of MOF structures.

5.2.3 The TBU Approach

Not only SBUs, but also larger molecular building units, can be used to design and synthesize complex MOF structures. If such building units are formed during the reticulation process, they are referred to as tertiary building units (TBUs) and examples for such TBUs are metal-organic polyhedra (MOPs, see Chapter 20). Such entities are formed *in situ* by linking of multiple individual building units (more precisely the segments of the organic linkers bearing the binding groups and the inorganic SBUs) into discrete 0D polyhedra. Here, the organic linker does not only connect adjacent SBUs, but also encodes the information for the *in situ* formation of the targeted TBU, thus enabling the design of structures built from "predefined" molecular cages. When analyzing the structure of MOP-1 (Cu_2(*m*-BDC)$_2$(H_2O)$_2$), a molecular polyhedron built from 4-c copper paddle wheel SBUs connected by *m*-BDC linkers, it becomes clear that multiple MOP-1 units can potentially be linked into a geometrically well-defined arrangement by functionalization of the isophthalate linkers to provide additional binding groups. This approach is illustrated in Figure 5.11 [16].

To allow for more predictability and thus the deliberate design of extended structures based on TBUs, nets of minimum transitivity that are exclusive for a certain combination of building units (vertex geometries) must be targeted. For the example shown in Figure 5.11 this means that in a first step the connectivity of the modified MOP-1 molecule needs to be determined. Each MOP-1 entity is built from 24 *m*-BDC linkers, and since the 5-positions of these linkers act as the points of extension, the truncated cuboctahedral MOP-1 TBU represent a 24-c rhombicuboctahedral (**rco**) vertex figure (Figure 5.11b). Such 24-c TBUs can form frameworks of **rht** topology (transitivity 2123) when linked by

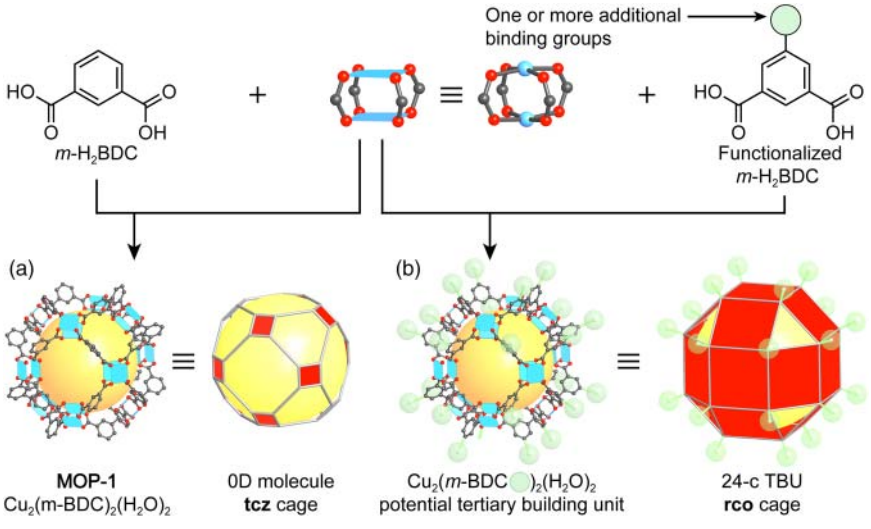

Figure 5.11 (a) Reticulation of *m*-H_2BDC linkers and 4-c Cu_2(—COO)$_4$ paddle wheel SBUs affords the formation of a discrete **tcz** cage. (b) Functionalization of the *m*-BDC linker in the 5-position yields a molecular building unit with 24 points of extension.

trigonal linkers. In the following text we will illustrate two strategies for linking MOP-1-based TBUs into 3D extended structures either through additional SBUs or deliberate linker design. When planning the synthesis of such compounds, it is important to keep in mind that the chemical nature of the linker must not interfere with the formation of the MOP-1 TBUs.

5.2.3.1 Linking TBUs Through Additional SBUs

A MOF constructed from rhombicuboctahedral TBUs linked through additional SBUs is **rht**-MOF-1 (Figure 5.12) [17]. Here, H_3TZI (5-tetrazolylisophthalic acid) is reticulated with Cu^{2+} ions. The isophthalate unit of the TZI linkers connects

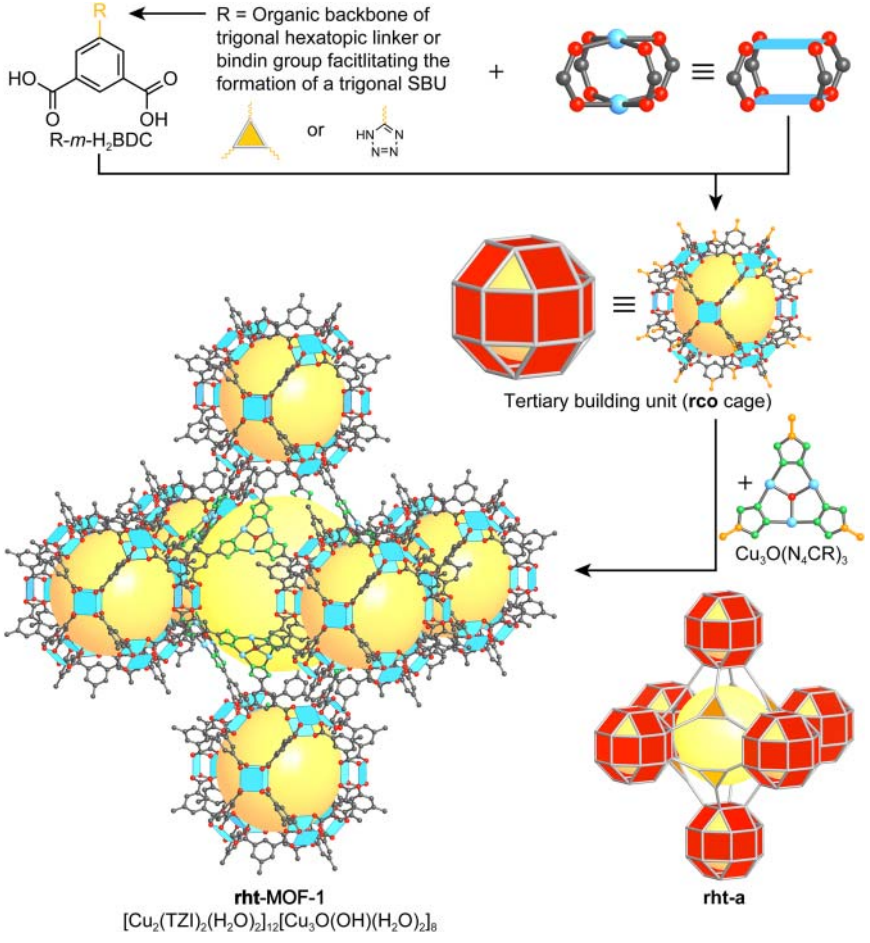

Figure 5.12 Crystal structure of **rht**-MOF-1. Copper paddle wheel SBUs are linked into MOP-1 TBUs (**tcz)** through the isophthalate segment of the H_2TZI linker. The tetrazole moieties installed at the 5-position of the isophthalate (C5 and C6 of the linker are highlighted in orange) are linked into trigonal $Cu_3OL_3(TZI)_3$ SBUs (D_{3h}) that connect the TBUs to yield an extended 3D structure of **rht** topology. The topology representation of the **rco** cage as well as the overall **rht** topology are shown. All hydrogen atoms are omitted for clarity. Color code: Cu, blue; C, gray; N, green; O, red.

two copper centers to form $Cu_2(-COO)_4$ paddle wheel SBUs thus yielding 24-c cuboctahedral TBUs bearing tetrazole group in the 5-position of each bridging isophthalate unit. The additional tetrazole binding groups are located precisely on the vertices of the rhombicuboctahedral TBUs and consequently each TBU is connected to 12 neighboring TBUs through 3-c $Cu_3OL_3(TZI)_3$ SBUs formed by linking three tetrazole groups of three adjacent TBUs [17a]. This affords a 3,24-connected structure with an overall **rht** topology. The structure encompasses three differently sized pores of **tcz**, **tcu**, and **rdo-a** topology. By identifying the two different types of SBU and the tritopic TZI linker as the building units of this MOF, its structure can also be described by the 3,3,4-connected **ntt** net; however, the resulting structure description is more complicated (see Figure 2.17).

For the deconstruction of the crystal structures of **rht**-MOFs in terms of an **rht** net, selecting the carbonyl carbons as the points of extension is not helpful and it is more meaningful to define new points of extension that help in simplifying the structure. In the example above, the 5-position of the isophthalate terminus provides the connection to neighboring TBUs; hence, from a topological point of view, a description of the isophthalate as having two points of extension is not meaningful and the description of isophthalate as one point of extension, located at its 5-position, is the more appropriate choice.

A general principle that describes the influence of linker terminus (e.g. isophthalate in the case of **rht**-MOF-1) on the hierarchical pore system, facilitates the design of **rht**-MOFs with tailored pore sizes. Changing the distance between the two carboxylate binding groups affords a framework with expanded TBUs (**tcz** cage, see linker of **rht**-MOF-2 in Figure 5.13) whereas changing the distance between the tetrazolate and the isophthalate segments leads to the expansion of the **rdo-a** and **tcu** cages (see linker of **rht**-MOF-3 in Figure 5.13).

5.2.3.2 Linking TBUs Through Organic Linkers

In an analogous fashion, purely organic linkers of appropriate symmetry can be used to prepare **rht**-MOFs. Such linkers are commonly composed of three isophthalate units joined through a core unit with trigonal symmetry. Here we will discuss a MOF with **rht** topology that is built from 24-c cuboctahedral TBUs and a trigonal hexatopic linker, H_6TTATP (5,5′,5″-(1,3,5-triazine-2,4,6-triyl)tris(azanediyl)triisophthalic acid). The molecular structure of H_6TTATP is composed of a triazine core unit connected to three isophthalate binding groups through secondary amines (see linker of **rht**-MOF-7 in Figure 5.13). Reticulation of Cu^{2+} ions with this linker leads to the *in situ* formation of MOP-1 TBUs that are consequently linked into an **rht** framework. In contrast to **rht**-MOP-1, a second SBU is not needed for the formation of **rht**-MOF-7. The metrics of all **rht**-MOFs can be modified following the same general design principles outlined earlier for tetrazole-based **rht**-MOFs. Different organic units of suitable geometry can be employed as the core of the hexatopic linker, which allows for the synthesis of isoreticular **rht**-MOFs with a wide variety of pore sizes (Figure 5.13) [17b].

The assembly of discrete metal-organic TBUs facilitates the rational design and synthesis of complex MOF structures, and MOPs appear to be ideal building units in this approach. Their high connectivity reduces the number of

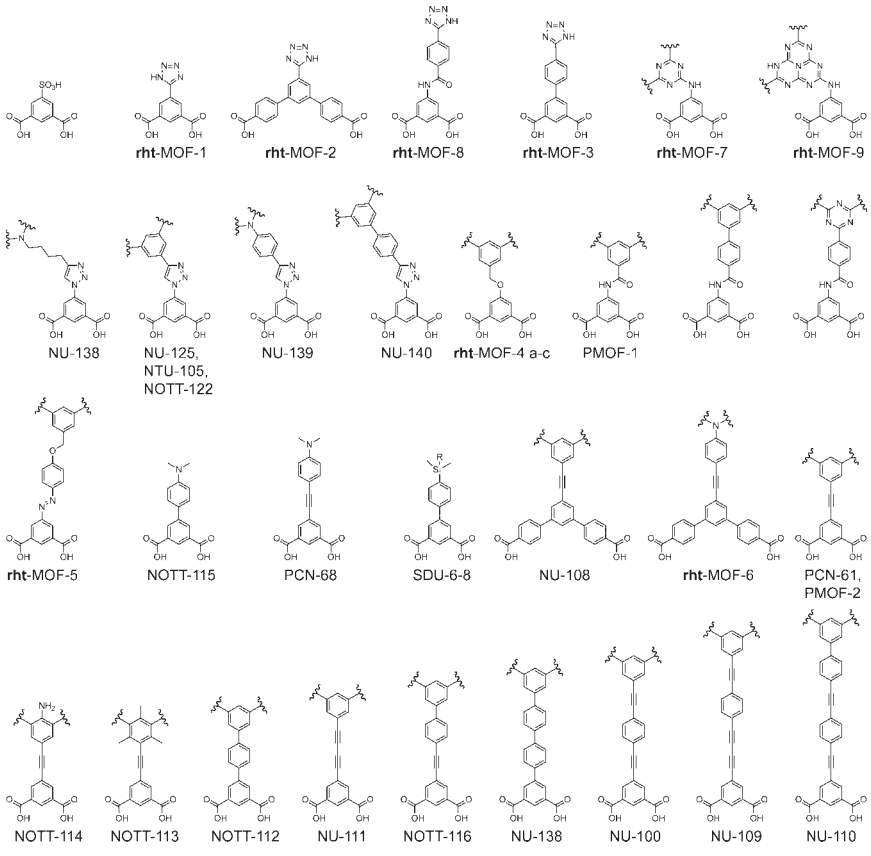

Figure 5.13 Compilation of linkers used in the preparation of MOFs with **rht** topology. Sulfonic acid and tetrazole derivatives rely on the *in situ* formation of trigonal SBUs to link up the individual TBUs. A variety of extending units have been used, and the largest linker affording a framework with **rht** topology (NU-110) is shown on the far bottom right corner.

accessible topologies when linked up into 3D frameworks and thus increases the predictability with respect to the targeted structure. Additionally, the high connectivity of such TBUs allows for the formation of framework structures that cannot be accessed otherwise. In analogy to the examples discussed in this chapter, a variety of different MOPs can be used as TBUs to yield highly complex MOFs [18, 19]. For a more detailed review on such MOFs the reader is referred elsewhere [17b, 19].

5.3 Heterogeneity in Frameworks

In contrast to framework complexity, heterogeneity is introduced through the presence of (i) multiple interchangeable linkers, with similar chemical behavior and metrics, but different chemical composition, (ii) multiple metal ions forming the same type of SBU, or (iii) aperiodic vacancies within the same structure.

Such MTV systems possess the same overall topology as the parent MOF. Since these structures feature at least two building units that have no topological preference as to what position in the crystal structure they occupy, these "elements of heterogeneity" result in an undefined spatial arrangement. This means that the possible emerging sequences are a result of the chemical nature of the individual constituents and the reaction conditions. Interestingly, phase separation is typically not observed and pure phase MTV-MOFs can be prepared from an appropriate mixture of starting materials. In the following text we will elaborate three approaches to introduce heterogeneity into frameworks: (i) mixed-linker MTV-MOFs, (ii) mixed-metal MTV-MOFs, and (iii) disordered vacancies.

5.3.1 Multi-Linker MTV-MOFs

MTV-MOF-5 marks the first report of a multivariate MOF. Here, a variety of X-H_2BDC derivatives (X = H, NH_2, Br, $(Cl)_2$, NO_2, $(CH_3)_2$, C_4H_4, $(OC_3H_5)_2$, and $(OC_7H_7)_2$) were implemented into the backbone of MOF-5 (Figure 5.14) [4]. To prepare such materials, a mixture of up to eight differently substituted X-H_2BDC linkers is employed in the synthesis of a single MOF. The resulting materials are isostructural to MOF-5 and possess both, the crystallinity and microporosity inherent to the parent MOF-5. Because the atomic coordinates of the BDC backbone of all linkers within the structure of MOF-5 are related by symmetry (MTV-MOF-5 crystallizes in the space group $Fm\bar{3}m$), the distribution of differently substituted linkers within the framework structure cannot be fully elucidated by diffraction techniques. Different scenarios may be envisioned for the arrangement of linkers within MTV-MOF-5: (i) a random distribution, (ii) a well-ordered alternating pattern, or (iii) clustering of functionalities. A combination of solid-state MAS NMR studies and molecular dynamics simulations can help to elucidate the determination of the apportionment differently substituted linkers within this structure. While some functionalities favor the formation of small clusters (e.g. $-NH_2$ and $-CH_3$), other functionalities prefer a random arrangement (e.g. $-NO_2$, $-(OC_3H_5)_2$, and $-(OC_7H_7)_2$), which suggests that the distribution of functionalities is highly dependent on their chemical nature. Interestingly, MTV-MOF-5 materials show gas adsorption properties superior to those of the parent MOF-5, an observation that is explained by the larger number of adsorption sites within the pores of the MTV system. A similar nonlinear enhancement of properties has been reported for other MTV systems [20].

5.3.2 Multi-Metal MTV-MOFs

Another approach to the synthesis of MTV-MOFs is the introduction of different metals on symmetry-equivalent sites within the SBUs, thus introducing heterogeneity into the backbone of the MOF. This is achieved either by a one-pot reaction or by post-synthetic metal exchange reactions (see Chapter 6). Co-doped mixed-metal (Zn)MOF-5:Co^{2+} containing 8 and 21% of cobalt is prepared in a one-pot reaction and while the incorporation of Co^{2+} into the zinc SBUs of the framework can be confirmed, the precise spatial distribution of Co^{2+} cannot be

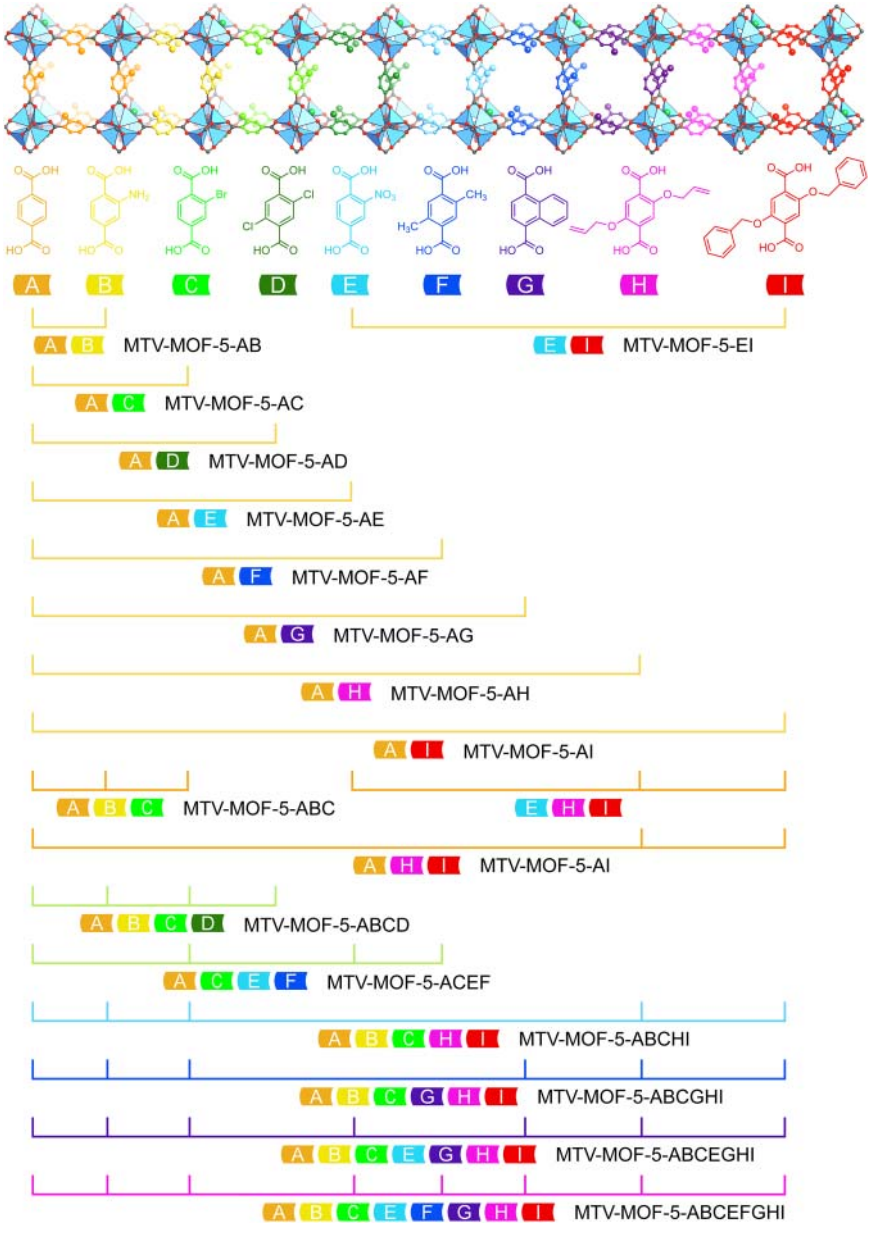

Figure 5.14 Different linker combinations used to prepare MTV-MOF-5. Up to eight chemically distinct BDC derivatives are employed in the syntheses yielding MTV-MOF-5 materials that encompass heterogeneous pore environments.

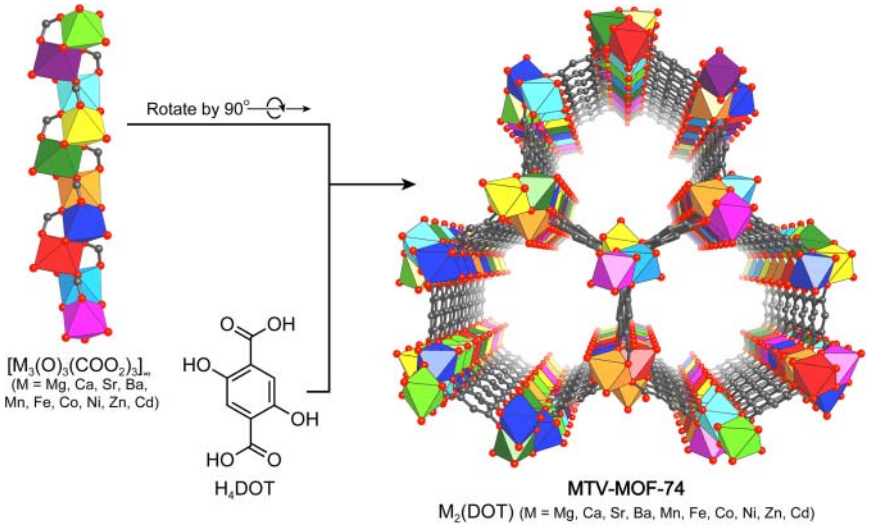

Figure 5.15 Crystal structure representation of MTV-MOF-74 with view along the crystallographic *c*-axis. The **etb** framework is formed by linking 1D $[M_3(O)_3(COO)_3]_\infty$ rod SBUs through DOT linkers. The resulting framework has hexagonal 1D channels running along the crystallographic *c*-axis. The SBUs of MTV-MOF-74 contain up to 10 different metals (Mg, Ca, Sr, Ba, Mn, Fe, Ni, Co, Zn, and Cd), out of which there are metals not present in binary MOF-74 structures. The metals are shown as their respective coordination polyhedra, each color represents a different metal. All hydrogen atoms are omitted for clarity. Color code: C, gray; O, red.

determined [21]. Mixed-metal analogs of MOF-5 containing Ti^{3+}, $V^{2+/3+}$, $Cr^{2+/3+}$, Mn^{2+}, and Fe^{2+} can be prepared by post-synthetic metal exchange reactions [22]. To incorporate trivalent metals, these are introduced in a reduced oxidation state and subsequently oxidized without effecting the original structure, crystallinity, and porosity of MOF-5.

Up to 10 different metals (Mg, Ca, Sr, Ba, Mn, Fe, Co, Ni, Zn, and Cd) can be incorporated into the SBUs of MOF-74 in a one-pot reaction yielding MTV-MOF-74 (Figure 5.15) [23]. This method allows to incorporate metal ions that cannot be employed in the synthesis of the pure phase MOF (i.e. Ca, Sr, Ba, and Cd). The determination of the spatial distribution of metal ions within such heterogeneous structures is a difficult task. Energy dispersive X-ray spectroscopy can help to elucidate the distribution of metal centers within such mixed-metal MOFs. Using this method, the distribution of different metals in the SBUs of MTV-MOF-74 was shown to be nonuniform.

Another example of mixed-metal MTV-MOFs are compounds of the general formula $[M_3OL_3]_2(TCPP\text{-}M)_3$, built from trinuclear $M_3OL_3(-COO)_6$ SBUs connected through tetratopic porphyrin-based linkers [24]. Using five different metals to construct the SBUs of the MOF and six different linkers (unmetalated TCPP-H_2 and five metalated derivatives TCPP-M) 36 isostructural MOFs of the general formula $[M_3OL_3]_2(TCPP\text{-}M)_3$ can be prepared (Figure 5.16). For the resulting structures, two scenarios arise: (i) formation of domains, i.e. different SBUs, each of which is composed of one sort of metal, form domains within the

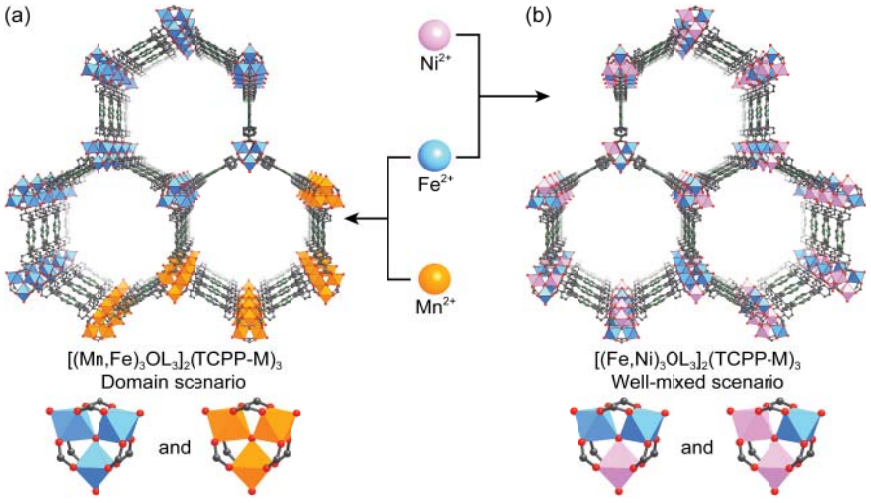

Figure 5.16 Crystal structure of $[M_3OL_3]_2(TCPP\text{-}M)_3$ with an underlying **stp** topology. (a) Metals with significantly different radii and electronegativity (Mn^{2+} and Fe^2) tend to form SBUs containing only one kind of metal, which results in a domain arrangement (b) Metals of similar radius and electronegativity (Fe^{2+} and Ni^{2+}) form mixed-metal SBUs, resulting in a well-mixed arrangement.

MOF structure and (ii) the well-mixed case, where different metals are present within the same SBU and the MOF structure is built from only mixed-metal SBUs. For all materials prepared in the way described earlier, no phase separation is observed as evidenced by energy dispersive X-ray spectroscopy, which is indicative of the formation of the targeted mixed-metal MTV-MOFs. As a general principle, metals of similar radius and electronegativity form mixed-metal SBUs (well-mixed arrangement), whereas metals with significantly different radii and electronegativity form SBUs built from one kind of metal (domain arrangement). This is well in accordance with the principles established for intermetallic or ionic solid-state materials and can experimentally be assessed by X-ray photoelectron spectroscopy.

5.3.3 Disordered Vacancies

Similar to the formation of MTV systems constructed from linkers bearing multiple different functionalities or mixed-metal centers within the SBU, the introduction of defects into a MOF structure can also yield an MTV system [25]. Furthermore, the presence of defects can enhance the properties of MOFs with respect to certain applications.

To illustrate this approach, we take a closer look at defects in the structure of UiO-66. Here, defects can be introduced by adding a strong modulator, such as trifluoroacetic acid, to the reaction mixture. During framework formation, the modulator competes with the BDC linker for binding sites on the SBU, resulting in missing linker defects whose presence can be verified by X-ray diffraction techniques [26]. Interestingly, the resulting defect rich material shows an

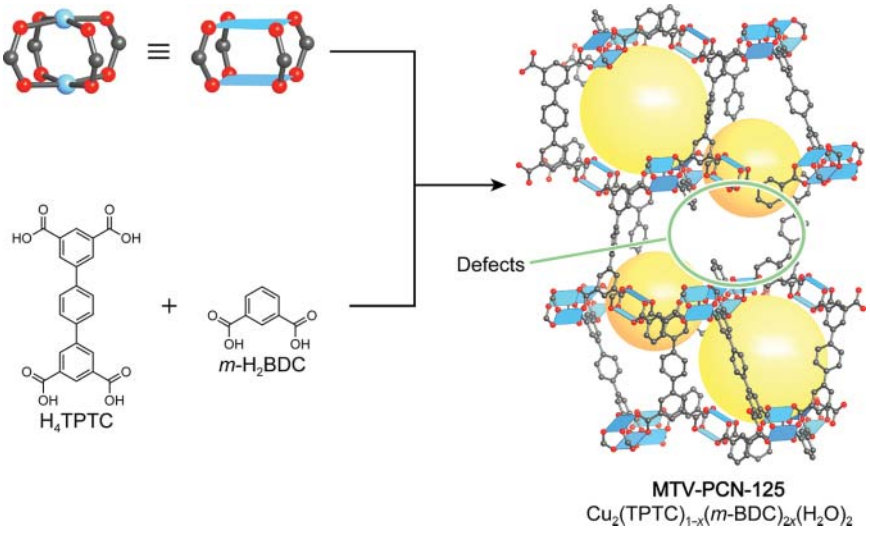

Figure 5.17 Disordered defects in the structure of PCN-125. The defects are introduced by adding *m*-H_2BDC to the reaction mixture. Even though defects are present in the structure, the material is crystalline. Disordered vacancies impart the pores with heterogeneity.

increased catalytic activity in the cyclization of citonellal to isopulegol compared to pristine UiO-66 and a similar enhancement of the properties of other defect rich MOFs is known [27]. Modulators used to introduce defect sites are often structurally related to the linker molecules used in the synthesis [25, 28]. An example making use of this strategy is the formation of defect rich PCN-125 ($[Cu_2(H_2O)_2]$(TPDC)) [28a]. Here, *m*-H_2BDC is added to the reaction mixture of Cu^{2+} ions and H_4TPTC to introduce missing-linker defects (Figure 5.17). Even though the resulting material displays a powder X-ray diffraction pattern identical to that of pristine PCN-125, the presence of *m*-BDC in the defect structure can be corroborated by digestion NMR. A schematic drawing of PCN-125 showing the nature of these defects is given in Figure 5.17. The presence of defects in PCN-125 increases the CO_2 uptake capacity which is attributed to the increased pore size of defect rich PCN-125. In a manner akin, defects can be introduced into other MOF structures [25, 28b].

Another approach to introducing defects is the rapid formation of MOF by fast precipitation [29]. Typical solvothermal reactions that yield single crystalline materials require reaction times of more than 12 hours, and fast crystal formation (<1 minute) is therefore expected to result in materials containing many defect sites [30].

A unique method for the preparation of MTV-MOFs with homogeneous pore sizes is micro-mesoporous MOF-5. By addition of DBA (4-(dodecycloxy)benzoic acid) to the reaction mixture, pomegranate-like crystals of pmg-MOF-5 consisting of a mesoporous core and a microporous shell are formed. Further increasing the amount of DBA in the reaction mixture even results in meso, macroporous sponge-like crystals [31].

Thus far, we only discussed the direct synthesis of MOFs providing us with the concepts of design in terms of the topology and metrics of MOF structures. However, another great advantage of MOFs over other porous materials is that their molecular building units can be addressed like molecules even though they are part of an extended solid. In Chapter 6, we will discuss ways to modify MOFs in terms of their structure and functionality to tailor the properties of a given material toward specific applications.

5.4 Summary

In this chapter we showed that MOFs built from more than two distinct building units can be classified as "complex" or "heterogeneous" and we made this distinction based on the crystallographic order of the backbone of the structure; the different positions the building units occupy within the structure. We showed MOF structures illustrating both concepts and derived general ways for constructing such structures. The expansion of the scope of structure accessible using the mixed-linker, mixed-metal, or MTV approach was highlighted and we saw that heterogeneity within frameworks can result in enhanced materials properties compared to the simple binary counterparts. Thus far, we discussed the direct synthesis of MOF by linking individual building units. The porous nature of MOFs further allows for the modification of their structures post-synthetically as well as for the formation of well-defined composite materials, and such modification and functionalization reactions will be the focus of Chapter 6.

References

1 (a) Li, H., Eddaoudi, M., O'Keeffe, M., and Yaghi, O.M. (1999). Design and synthesis of an exceptionally stable and highly porous metal-organic framework. *Nature* 402 (6759): 276–279. (b) Furukawa, H., Ko, N., Go, Y.B. et al. (2010). Ultrahigh porosity in metal-organic frameworks. *Science* 329 (5990): 424–428.

2 Koh, K., Wong-Foy, A.G., and Matzger, A.J. (2008). A crystalline mesoporous coordination copolymer with high microporosity. *Angewandte Chemie International Edition* 47 (4): 677–680.

3 Eddaoudi, M., Kim, J., Rosi, N. et al. (2002). Systematic design of pore size and functionality in isoreticular MOFs and their application in methane storage. *Science* 295 (5554): 469–472.

4 Deng, H., Doonan, C.J., Furukawa, H. et al. (2010). Multiple functional groups of varying ratios in metal-organic frameworks. *Science* 327 (5967): 846–850.

5 Schnobrich, J.K., Lebel, O., Cychosz, K.A. et al. (2010). Linker-directed vertex desymmetrization for the production of coordination polymers with high porosity. *Journal of the American Chemical Society* 132 (39): 13941–13948.

6 Tranchemontagne, D.J., Park, K.S., Furukawa, H. et al. (2012). Hydrogen storage in new metal-organic frameworks. *The Journal of Physical Chemistry C* 116 (24): 13143–13151.

7 Chui, S.S.-Y., Lo, S.M.-F., Charmant, J.P.H. et al. (1999). A chemically functionalizable nanoporous material $[Cu_3(TMA)_2(H_2O)_3]_n$. *Science* 283 (5405): 1148–1150.

8 Tu, B., Pang, Q., Ning, E. et al. (2015). Heterogeneity within a mesoporous metal-organic framework with three distinct metal-containing building units. *Journal of the American Chemical Society* 137 (42): 13456–13459.

9 Koh, K., Wong-Foy, A.G., and Matzger, A.J. (2010). Coordination copolymerization mediated by $Zn_4O(CO_2R)_6$ metal clusters: a balancing act between statistics and geometry. *Journal of the American Chemical Society* 132 (42): 15005–15010.

10 Koh, K., Wong-Foy, A.G., and Matzger, A.J. (2009). A porous coordination copolymer with over 5000 m^2/g BET surface area. *Journal of the American Chemical Society* 131 (12): 4184–4185.

11 (a) Lee, S.J., Doussot, C., and Telfer, S.G. (2017). Architectural diversity in multicomponent metal-organic frameworks constructed from similar building blocks. *Crystal Growth & Design* 17 (6): 3185–3191. (b) Grunker, R., Bon, V., Muller, P. et al. (2014). A new metal-organic framework with ultra-high surface area. *Chemical Communications* 50 (26): 3450–3452.

12 Dutta, A., Wong-Foy, A.G., and Matzger, A.J. (2014). Coordination copolymerization of three carboxylate linkers into a pillared layer framework. *Chemical Science* 5 (10): 3729–3734.

13 Liu, L., Konstas, K., Hill, M.R., and Telfer, S.G. (2013). Programmed pore architectures in modular quaternary metal-organic frameworks. *Journal of the American Chemical Society* 135 (47): 17731–17734.

14 Liu, L. and Telfer, S.G. (2015). Systematic ligand modulation enhances the moisture stability and gas sorption characteristics of quaternary metal-organic frameworks. *Journal of the American Chemical Society* 137 (11): 3901–3909.

15 Yuan, S., Lu, W., Chen, Y.-P. et al. (2015). Sequential linker installation: precise placement of functional groups in multivariate metal-organic frameworks. *Journal of the American Chemical Society* 137 (9): 3177–3180.

16 Eddaoudi, M., Kim, J., Wachter, J.B. et al. (2001). Porous metal-organic polyhedra: 25 Å cuboctahedron constructed from 12 $Cu_2(CO_2)_4$ paddle-qheel building blocks. *Journal of the American Chemical Society* 123 (18): 4368–4369.

17 (a) Nouar, F., Eubank, J.F., Bousquet, T. et al. (2008). Supermolecular building blocks (SBBs) for the design and synthesis of highly porous metal-organic frameworks. *Journal of the American Chemical Society* 130 (6): 1833–1835. (b) Eubank, J.F., Nouar, F., Luebke, R. et al. (2012). On demand: the singular rht net, an ideal blueprint for the construction of a metal-organic framework (MOF) platform. *Angewandte Chemie International Edition* 51 (40): 10099–10103. (c) Luebke, R., Eubank, J.F., Cairns, A.J. et al. (2012). The unique rht-MOF platform, ideal for pinpointing the functionalization and CO_2 adsorption relationship. *Chemical Communications* 48 (10): 1455–1457. (d) Pham, T., Forrest, K.A., Hogan, A. et al. (2014). Simulations of hydrogen sorption in rht-MOF-1: identifying the binding sites through explicit polarization and quantum rotation calculations. *Journal of Materials Chemistry A* 2 (7): 2088–2100.

18 (a) Zheng, B., Bai, J., Duan, J. et al. (2010). Enhanced CO_2 binding affinity of a high-uptake rht-type metal-organic framework decorated with acylamide groups. *Journal of the American Chemical Society* 133 (4): 748–751. (b) Yuan, D., Zhao, D., Sun, D., and Zhou, H.C. (2010). An isoreticular series of metal-organic frameworks with dendritic hexacarboxylate ligands and exceptionally high gas-uptake capacity. *Angewandte Chemie International Edition* 49 (31): 5357–5361. (c) Farha, O.K., Yazaydın, A.Ö., Eryazici, I. et al. (2010). De novo synthesis of a metal-organic framework material featuring ultrahigh surface area and gas storage capacities. *Nature Chemistry* 2 (11): 944–948.

19 Guillerm, V., Kim, D., Eubank, J.F. et al. (2014). A supermolecular building approach for the design and construction of metal-organic frameworks. *Chemical Society Reviews* 43 (16): 6141–6172.

20 (a) Park, T.-H., Koh, K., Wong-Foy, A.G., and Matzger, A.J. (2011). Nonlinear properties in coordination copolymers derived from randomly mixed ligands. *Crystal Growth & Design* 11 (6): 2059–2063. (b) Zhang, Y.-B., Furukawa, H., Ko, N. et al. (2015). Introduction of functionality, selection of topology, and enhancement of gas adsorption in multivariate metal-organic framework-177. *Journal of the American Chemical Society* 137 (7): 2641–2650.

21 Botas, J.A., Calleja, G., Sánchez-Sánchez, M., and Orcajo, M.G. (2010). Cobalt doping of the MOF-5 framework and its effect on gas-adsorption properties. *Langmuir* 26 (8): 5300–5303.

22 Brozek, C.K. and Dincă, M. (2013). Ti^{3+}-, $V^{2+/3+}$-, $Cr^{2+/3+}$-, Mn^{2+}-, and Fe^{2+}-aubstituted MOF-5 and redox reactivity in Cr- and Fe-MOF-5. *Journal of the American Chemical Society* 135 (34): 12886–12891.

23 Wang, L.J., Deng, H., Furukawa, H. et al. (2014). Synthesis and characterization of metal-organic framework-74 containing 2, 4, 6, 8, and 10 different metals. *Inorganic Chemistry* 53 (12): 5881–5883.

24 Liu, Q., Cong, H., and Deng, H. (2016). Deciphering the spatial arrangement of metals and correlation to reactivity in multivariate metal-organic frameworks. *Journal of the American Chemical Society* 138 (42): 13822–13825.

25 Fang, Z., Dürholt, J.P., Kauer, M. et al. (2014). Structural complexity in metal-organic frameworks: simultaneous modification of open metal sites and hierarchical porosity by systematic doping with defective linkers. *Journal of the American Chemical Society* 136 (27): 9627–9636.

26 (a) Wu, H., Chua, Y.S., Krungleviciute, V. et al. (2013). Unusual and highly tunable missing-linker defects in zirconium metal-organic framework UiO-66 and their important effects on gas adsorption. *Journal of the American Chemical Society* 135 (28): 10525–10532. (b) Cliffe, M.J., Wan, W., Zou, X. et al. (2014). Correlated defect nano-regions in a metal-organic framework. *Nature Communications* 5: 4176.

27 Vermoortele, F., Bueken, B., Le Bars, G. et al. (2013). Synthesis modulation as a tool to increase the catalytic activity of metal-organic frameworks: the unique case of UiO-66(Zr). *Journal of the American Chemical Society* 135 (31): 11465–11468.

28 (a) Park, J., Wang, Z.U., Sun, L.-B. et al. (2012). Introduction of functionalized mesopores to metal-organic frameworks via metal–ligand–fragment coassembly. *Journal of the American Chemical Society* 134 (49): 20110–20116.
(b) Barin, G., Krungleviciute, V., Gutov, O. et al. (2014). Defect creation by linker fragmentation in metal-organic frameworks and its effects on gas uptake properties. *Inorganic Chemistry* 53 (13): 6914–6919.

29 Ravon, U., Savonnet, M., Aguado, S. et al. (2010). Engineering of coordination polymers for shape selective alkylation of large aromatics and the role of defects. *Microporous and Mesoporous Materials* 129 (3): 319–329.

30 Huang, L., Wang, H., Chen, J. et al. (2003). Synthesis, morphology control, and properties of porous metal-organic coordination polymers. *Microporous and Mesoporous Materials* 58 (2): 105–114.

31 Choi, K.M., Jeon, H.J., Kang, J.K., and Yaghi, O.M. (2011). Heterogeneity within order in crystals of a porous metal-organic framework. *Journal of the American Chemical Society* 133 (31): 11920–11923.